ISSN 0020-1685, Inorganic Materials, 2007, Vol. 43, No. 7, pp. 704–710. © Pleiades Publishing, Inc., 2007.
Original Russian Text © S.A. Lushnikov, A.M. Balagurov, I.A. Bobrikov, V.N. Verbetsky, V.P. Glazkov, V.A. Somenkov, 2007, published in Neorganicheskie Materialy, 2007, Vol. 43, No. 7, pp. 797–804.

Synthesis and Structure of $CeNi_3D_x$

S. A. Lushnikov[a], A. M. Balagurov[b], I. A. Bobrikov[b], V. N. Verbetsky[a], V. P. Glazkov[c], and V. A. Somenkov[c]

[a] *Moscow State University, Vorob'evy gory 1, Moscow, 119992 Russia*
[b] *Joint Institute for Nuclear Research, ul. Zholio-Kyurie 6, Dubna, Moscow oblast, 141980 Russia*
[c] *Russian Research Centre Kurchatov Institute, pl. Kurchatova 1, Moscow, 123182 Russia*
e-mail: lushnikov@hydride.chem.msu.ru

Received September 28, 2006

Abstract—We describe the synthesis of $CeNi_3D_x$ deuterides at normal and high deuterium pressures. X-ray and neutron diffraction techniques were used to identify the position and determine the positional parameters of the metal and deuterium atoms. The deuterides are isostructural with the parent compound $CeNi_3$ but have a larger unit cell. Increasing the deuterium content to the composition $CeNi_3D_{5.2}$ leads to partial amorphization of the material. The variation in unit-cell volume observed at low and high deuterium contents indicates that the metal–deuterium bonds are partially ionic and partially metallic.

DOI: 10.1134/S0020168507070060

INTRODUCTION

Knowledge of the general mechanisms responsible for the hydrogen-induced structural and volume changes in hydrides of transition metals and alloys is crucial for understanding the bonding configuration in these compounds and predicting their potential technological applications. In studies of the interaction between intermetallic compounds and hydrogen, particular interest has been centered on RT_3 (R = rare-earth metal, T = transition metal) compounds having $PuNi_3$, $CeNi_3$, and related structures. Their structure is commonly thought of as made up of blocks of well-known compounds with the RT_2 ($MgZn_2$ structure) and RT_5 ($CaCu_5$ structure) stoichiometries, stacked along the *c* axis, and is intermediate between these two types of structures. As shown by a variety of characterization techniques, the hydriding of some compounds gives rise to a significant anisotropic lattice expansion, whereas other hydrides show insignificant lattice anisotropy. The origin of the anisotropy is not yet clear. Recent studies of the compounds CeY_2Ni_9 and LaY_2Ni_9 ($PuNi_3$ structure) [1] have shown that the hydrogen-induced lattice expansion in hydrided CeY_2Ni_9 is anisotropic and that the hydrogen is accommodated in the RT_2 blocks, whereas the lattice expansion in hydrided LaY_2Ni_9 is only slightly anisotropic, and the hydrogen resides in both the RT_2 and RT_5 blocks. The Ce valence was shown to decrease insignificantly, so that the associated increase in its metallic radius cannot account for the anisotropic expansion of the hydride lattice. At the same time, $CeNi_3$ hydrided at low hydrogen pressures was reported to experience considerable anisotropic lattice expansion, up to 30% along the *c* axis, with insignificant changes in its in-plane lattice parameters [2–4]. As shown by Yartys et al. [5], the formation of the $CeNi_3D_{2.8}$ deuteride is accompanied by a reduction in lattice symmetry from hexagonal to orthorhombic, and most of the hydrogen atoms occupy new sites in the RT_2 block, which differ in metal coordination from the sites in the unit cell of the parent intermetallic compound. Verbetsky et al. [6] synthesized the $CeNi_3H_{5.6}$ hydride at high hydrogen pressures. X-ray diffraction (XRD) examination showed that the metal matrix retained its structural basis. Small lattice anisotropy was reported for hydrided $SmRu_{1.2}Co_{1.8}$ and $SmRu_{1.6}Ni_{1.4}$ ($CeNi_3$ structure) [7]. A structural study of $ErNi_3D_x$ with $x = 1.23$, 1.97, and 3.75 was reported by Filinchuk and Yvon [8]. Their results indicate that, at the lowest deuterium content ($ErNi_3D_{1.23}$), hydrogen is accommodated in the RT_2 block (positions $18h_7$ and $6c_1$), while increasing the deuterium content ($ErNi_3D_{1.97}$) causes hydrogen to occupy, in addition, positions common to the RT_2 and RT_5 blocks ($18h_2$) and also positions in the RT_5 block ($18h_8$). In the $ErNi_3D_{3.75}$ deuteride, hydrogen resides predominantly in the RT_2 block (positions $18h_7$, $18h_3$, and $6c_3$), while positions in the RT_5 block ($18h_8$) and between the blocks ($18h_2$) have lower occupancies.

Thus, previous work has made it possible to identify a number of factors, such as valence changes and hydrogen accommodation in different structural blocks, which shed some light on the nature of lattice distortion in hydrides, but the origin of the anisotropic lattice expansion in hydrides is not yet fully understood. In a recent structural study [9], hydrided $CeCo_3$ and $ErNi_3$ were shown to differ markedly in lattice

Table 1. Composition, lattice parameters, and volume change of deuterided $CeNi_3$ and intermetallic hydrides

Composition	a, nm	b, nm	c, nm	$V \times 10^3$, nm^3	$\Delta V/V$, %	$(\Delta V/\mathrm{D}) \times 10^3$, nm^3
$CeNi_3$ [9]	0.4945(2)	–	1.648(2)	349	–	–
$CeNi_3$	0.4964(3)	–	1.653(1)	353	–	–
$CeNi_3D_{3.3}$	0.4934(2)	–	2.173(3)	458	29.7	5.3
$CeNi_3D_{5.2}$	0.4938(3)	–	2.244(1)	474	34.2	3.9 (1.4)*
$SmRu_{1.2}Co_{1.8}$ [7]	0.896	0.516	1.677	775	–	–
$SmRu_{1.6}Ni_{1.4}$ [7]	0.889	0.513	1.678	765	–	–
$SmRu_{1.2}Co_{1.8}H_{4.5}$ [7]	0.973	0.550	1.782	954	23	3.3
$SmRu_{1.6}Ni_{1.4}H_{3.3}$ [7]	0.911	0.552	1.806	908	19	3.6

Note: $\Delta V/\mathrm{D}$ is the increase in unit-cell volume per absorbed deuterium atom.
* The number in parentheses corresponds to the transition from the low- to high-pressure deuteride.

anisotropy, which was relatively strong in the case of the light rare earth and weak in the case of the heavy rare earth. The volume changes observed in hydrided $CeCo_3$ and $ErNi_3$ agree well with the lattice expansion data for binary hydrides of rare earths and transition metals [10]. To interpret the different hydriding behaviors of these intermetallic compounds, it was hypothesized that there were different hydrogen–metal bonds: predominantly ionic for the rare-earth metals (donor behavior of hydrogen) and predominantly metallic for the transition metals (acceptor behavior of hydrogen), with emptying of the *sp* band and filling of the *d* band. That hypothesis might also be relied on in interpreting the large lattice anisotropy in $CeNi_3$, after determining the hydrogen positions in the structures of hydrogen-rich and hydrogen-poor hydrides. Calculations reported by Yartys [4] indicate that the highest hydrogen content of RT_3 intermetallic hydrides is 5.6–6.0 hydrogen atoms per formula unit. Therefore, using high-pressure synthesis, one can prepare hydrides with different hydrogen contents in which hydrogen is accommodated in both types of structural blocks.

In this paper, we report a structural study of $CeNi_3$ hydrided at normal and high hydrogen pressures.

EXPERIMENTAL

The $CeNi_3$ alloy was prepared by arc-melting pure metals in an inert atmosphere and was then annealed at 1020 K for 240 h in an evacuated silica tube. Deuterides were synthesized in a high-pressure apparatus (p_{D_2} up to 0.2 GPa [11]) and at low pressure ($p_{D_2} \le 0.01$ GPa) in a Sieverts apparatus. To avoid the formation of x-ray amorphous materials in the low-pressure synthesis, deuterium was introduced into the reactor in portions at a pressure $p_{D_2} \le 0.1$ MPa, and after each portion the reaction was given time to reach completion. After the low-pressure synthesis, the pressure in the system was gradually raised to the maximum level. To prevent deuterium losses, the synthesized deuterides were cooled and held at liquid-nitrogen temperature (77 K) in air. The amount of absorbed deuterium was determined by thermal desorption measurements.

Neutron diffraction measurements were performed on a DISK diffractometer ($\lambda = 0.166$ nm) at the Russian Research Centre Kurchatov Institute and on a high-resolution Fourier diffractometer at the Joint Institute for Nuclear Research using the time-of-flight technique. The diffraction data were analyzed using Fullprof and Mriya programs. The compositions of the deuterides determined by thermal desorption measurements differed insignificantly from those extracted from neutron diffraction data. XRD patterns were collected on Rigaku and ThermoARL diffractometers.

RESULTS AND DISCUSSION

According to our XRD and neutron diffraction results, the $ErNi_3$ alloy was single-phase, and its lattice parameters agreed with earlier data [12] (Table 1, Fig. 1a). The XRD and neutron diffraction data for the deuterides (Figs. 1b, 2) are in good agreement and show that the structures of the metal matrices of $CeNi_3D_{3.3}$ and $CeNi_3D_{5.2}$ can be represented by anisotropically expanded unit cells of the parent compound $CeNi_3$, with altered z coordinates of the metal atoms. The c cell parameter is increased by about 30%. In contrast to that of $CeNi_3D_{2.8}$, the XRD pattern of $CeNi_3D_{3.3}$ shows no peaks from the orthorhombic phase described by Yartys et al. [5]. The models of orthorhombic and hexagonal cells are very similar (and only differ in several weak XRD peaks, which may well be due to impurity phases) and are close in R_w, so that, in any case, the lattice distortion in going from $CeNi_5D_{2.8}$ to $CeNi_5D_{3.3}$ is not strong.

The neutron diffraction data for the deuterium-poor deuteride $CeNi_3D_{3.3}$ (Table 2, Fig. 3) indicate that the occupancies of positions $24l_1$, $24l_2$, and $12k_1$ are lower than that of position $4f_1$. Positions $24l_1$ and $12k_1$ (R_2T_2 coordination) contain more cerium (located

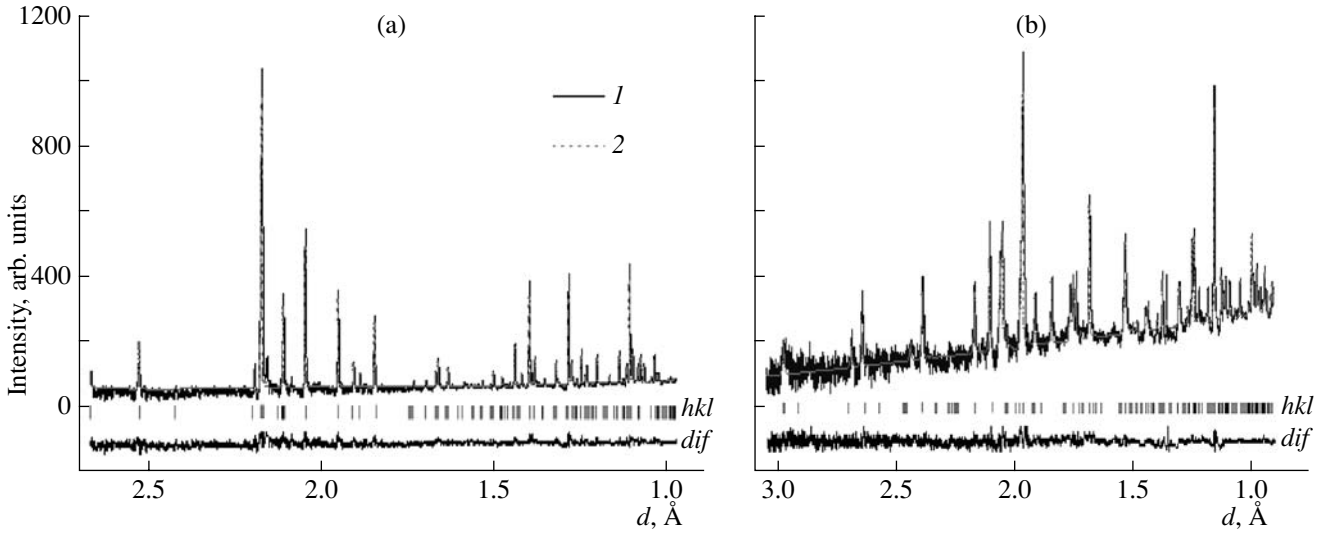

Fig. 1. Time-of-flight neutron diffraction patterns of (a) $CeNi_3$ and (b) $CeNi_3D_{3.3}$: (*1*) raw data, (*2*) calculated profile.

around interstices) than do positions $24l_2$ and $4f_1$ (RT_3 coordination). Positions $24l_1$ and $4f_1$ lie in the structural block RT_2, position $24l_2$ lies in the RT_5 block, and position $12k_1$ is shared by the RT_2 and RT_5 blocks. The structures of the deuterides inferred from the data collected on the DISK and high-resolution Fourier diffractometers differ only slightly in site occupancies and atomic coordinates. Increasing the deuterium content leads to partial amorphization of the metal matrix: the neutron diffraction pattern of $CeNi_3D_{5.2}$ shows a diffuse halo (Fig. 2). The presence of the amorphous phase impairs the accuracy of our structural data. In $CeNi_3D_{5.2}$ (Table 2, Fig. 3), the occupancies of the partially occupied positions $24l_1$, $24l_2$, $12k_1$, and $4f_1$ are higher, and the octahedral position $6h_1$ may be occupied.

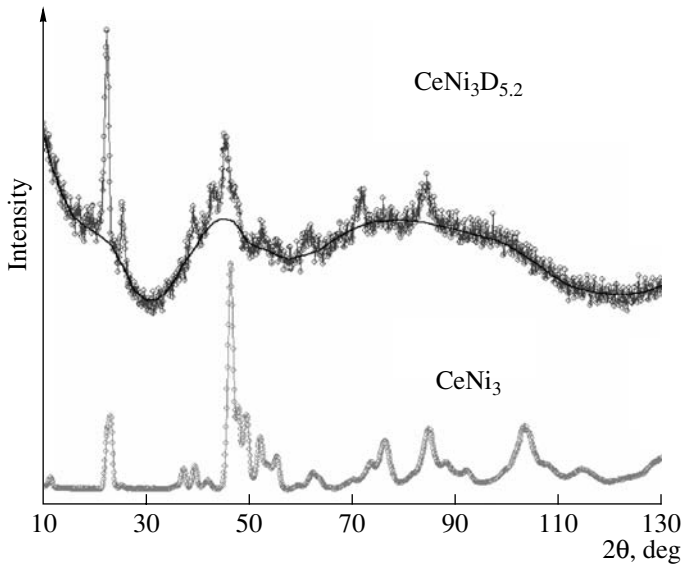

Fig. 2. Neutron diffraction pattern of $CeNi_3D_{5.2}$ in comparison with that of $CeNi_3$.

Comparison of bond lengths at different deuterium contents indicates that deuteriding increases the metal–metal bond lengths nonuniformly. In particular, the distance between the Ce atoms in position $24l_1$ in $CeNi_3D_{3.3}$ (Figs. 3, 4; Table 3) is 23% longer than that in the parent compound. In $CeNi_3D_{5.2}$, this bond length is 1% shorter in comparison with $CeNi_3D_{3.3}$ (0.318 ⟶ 0.392 ⟶ 0.389 nm). The Ce–Ni distance in both $CeNi_3D_{3.3}$ and $CeNi_3D_{5.2}$ is increased by 50%, attesting to bond breaking (0.314 ⟶ 0.470 ⟶ 0.469 nm). The Ce–Ni bond length in the basal plane in $CeNi_3D_{3.3}$ and $CeNi_3D_{5.2}$ is 7% longer than that in the parent compound (0.294 ⟶ 0.315 ⟶ 0.314 nm). The Ni–Ni distance in $CeNi_3D_{3.3}$ and $CeNi_3D_{5.2}$ is increased by 35%, which also indicates bond breaking (0.254 ⟶ 0.344 ⟶ 0.345 nm). The Ce–D bonds in $CeNi_3D_{3.3}$ are identical in length (0.250 nm), whereas the Ce–D bond length in $CeNi_3D_{5.2}$ depends on the type of Ce atom (0.210 and 0.299 nm), indicating that the deuterium atom is displaced toward the basal plane. The Ni–D bond lengths in $CeNi_3D_{3.3}$ and $CeNi_3D_{5.2}$ differ by no more than 2% (0.192 ⟶ 0.196 nm). Comparison of the bond lengths for the octahedral position $6h_1$ (Fig. 3, Table 3) demonstrates that the Ce–Ni bond length in the equatorial plane is the same (to within 1%) in the intermetallic compound, $CeNi_3D_{3.3}$, and $CeNi_3D_{5.2}$. At the same time, the distance between the Ni atoms at the vertices of the octahedron and the Ce atoms in the equatorial plane is increased by 6% in $CeNi_3D_{3.3}$ and by 9% in $CeNi_3D_{5.2}$ (0.320 ⟶ 0.338 ⟶ 0.349 nm). The distance between the Ni atoms at the vertices of the octa-

Table 2. Crystal data for deuterided $CeNi_3$

Atom	Position	Atoms per unit cell	x	y	z	Atoms per unit cell	x	y	z
		$CeNi_3D_{3.3}$				$CeNi_3D_{5.2}$			
Ce1	2c	2.0	0.333	0.666	0.25	2.0	0.333	0.666	0.25
Ce2	4f	4.0	0.333	0.666	0.061(2)	4.0	0.333	0.666	0.059(3)
Ni1	2a	2.0	0	0	0	2.0	0	0	0
Ni2	2b	2.0	0	0	0.25	2.0	0	0	0.25
Ni3	2d	2.0	0.333	0.666	0.75	2.0	0.333	0.666	0.75
Ni4	12k	12.0	0.833(2)	0.666(2)	0.146(1)	12.0	0.833(1)	0.666(1)	0.140(3)
D1	24l_2	6.0(1)	0.802(2)	0.137(1)	0.292(2)	10.3(3)	0.799(2)	0.138(3)	0.289(2)
D2	24l_1	10.1(2)	0.754(1)	0.666(2)	0.443(2)	13.9(2)	0.759(3)	0.669(2)	0.446(2)
D3	4f_1	1.3(1)	0.333	0.666	0.577(1)	0.8(3)	0.333	0.666	0.570(3)
D4	12k_1	3.6(2)	0.401(1)	0.802(1)	0.152(2)	4.9(3)	0.402(2)	0.804(2)	0.144(2)
D5	6h	–	–	–	–	2.4(4)	0.166(2)	0.833(2)	0.75
		R_p = 7.0%, R_w = 6.2%, R_B = 8.2%, D/FU = 3.5				R_p = 12.4%, R_w = 8.1%, R_B = 14.1%, D/FU = 5.4			

hedron and those in the equatorial plane is increased even more, by 14% in both $CeNi_3D_{3.3}$ and $CeNi_3D_{5.2}$ (0.249 ⟶ 0.285 ⟶ 0.285 nm). The octahedral site in question is occupied by deuterium only in $CeNi_3D_{5.2}$, but its volume is increased by 12% in $CeNi_3D_{3.3}$ and by 21% in $CeNi_3D_{5.2}$ (0.959×10^{-3} ⟶ 1.075×10^{-3} ⟶ 1.164×10^{-3} nm^3). Comparison of bond lengths in position 24l_2 of the structural block RT_5 (Figs. 3, 4; Table 3) demonstrates that the Ce–Ni bond length in the base of the tetrahedron varies little (by about 1%). At the same time, the distance between the apical Ni atom and the Ni atoms in the base is increased by 9% in $CeNi_3D_{3.3}$ and by 15% in $CeNi_3D_{5.2}$ (0.249 ⟶ 0.271 ⟶ 0.285 nm). The distance between the apical Ni and the Ce atom in the base is also increased: by 6% in $CeNi_3D_{3.3}$ and by 9% in $CeNi_3D_{5.2}$ (0.320 ⟶ 0.338 ⟶ 0.349 nm). As a result, the Ce–Ni bond in $CeNi_3D_{5.2}$ is considerably weaker. Thus, the metal matrix in the deuterium-rich compound $CeNi_3D_{5.2}$ contains an increased density of broken M–M bonds.

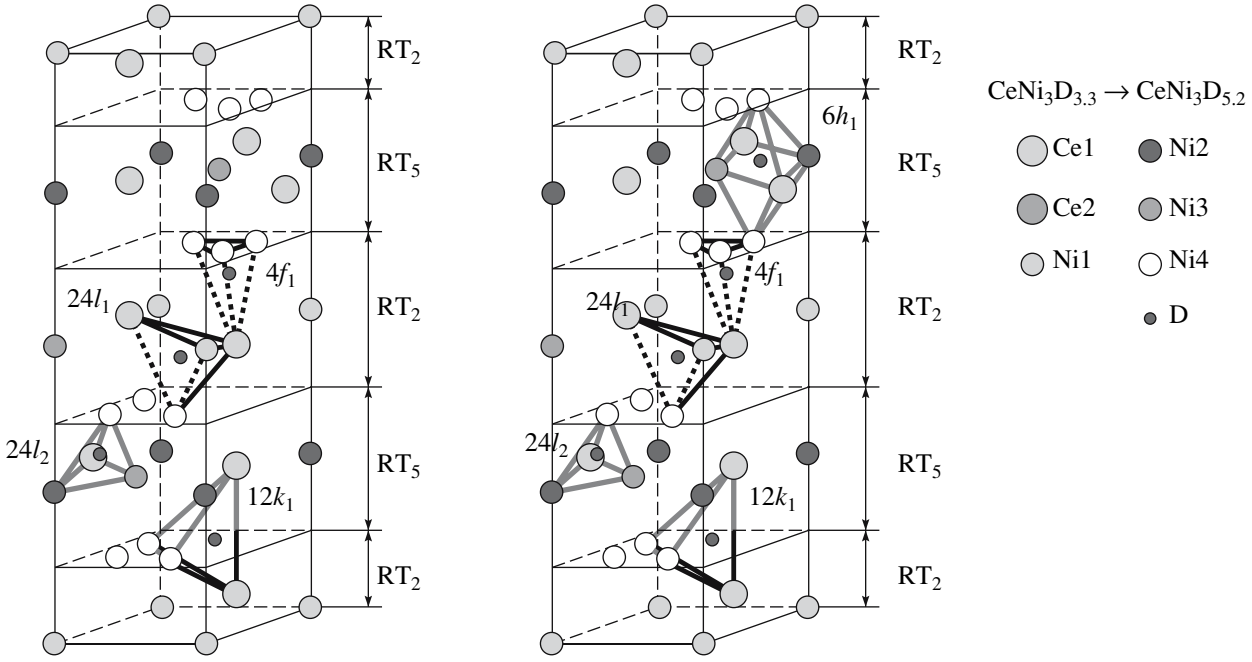

Fig. 3. Occupied sites in deuterided $CeNi_3$.

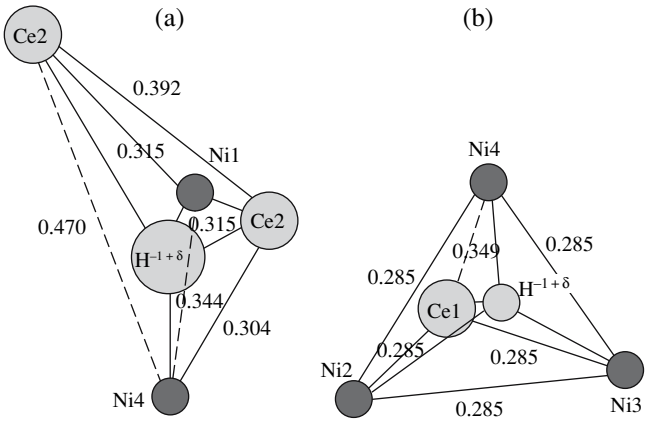

Fig. 4. Position of hydrogen atoms: (a) $CeNi_3D_{3.3}$, RT_2 block, position $24l_1$; (b) $CeNi_3D_{5.2}$, RT_5 block, position $24l_2$.

Comparison of the interstice radius in the tetrahedral position $24l_1$ of the $CeNi_3D_{3.3}$ and $CeNi_3D_{5.2}$ deuterides with that in $CeNi_3$ (Table 4) demonstrates that deuteriding increases it (0.04 ⟶ 0.07 ⟶ 0.11 nm). One should, however, keep in mind that, in the deuterides, the tetrahedron in this position is hypothetical (in comparison with the intermetallic compound) because of the breaking of some of the metal–metal bonds, as is the sphere inscribed in the tetrahedron, whose radius is taken to be the interstice radius. In $CeNi_3D_{3.3}$, the deuterium atom is displaced from the center position of the hypothetical tetrahedron toward the plane defined by two Ce atoms and one Ni atom (Fig. 3), and the Ce–D bonds are identical in length. In $CeNi_3D_{5.2}$, the deuterium atom is also displaced from the center position of the thought tetrahedron toward the plane defined by two Ce atoms and one Ni atom, but the Ce–D bonds differ in length. This implies that the Ce, Ni, and D atoms of the hypothetical tetrahedron are divided into groups, Ce–D and Ce–Ni, which belong to new chemical species formed through disproportionation at a higher temperature. Similarly, the interstice radius in the $6h_1$ octahedron (Table 4) changes insignificantly in going from the intermetallic compound to $CeNi_3D_{3.3}$ and to $CeNi_3D_{5.2}$ (0.019 ⟶ 0.018 ⟶ 0.019 nm). The deuterium atom in $CeNi_3D_{5.2}$ resides in

Table 3. Bond lengths in $CeNi_3$ and $CeNi_3D_x$

Position and structural block	Bond length, nm											
	$CeNi_3$			$CeNi_3D_{3.3}$				$CeNi_3D_{5.2}$				
$24l_2$	Ce1–Ni3	0.286		Ce1–Ni3	0.249	Ce1–D	0.278	Ce1–Ni3	0.285	Ce1–D	0.247	
RT_5	Ce1–Ni4	0.320		Ce1–Ni4	0.338	Ni2–D	0.171	Ce1–Ni4	0.349	Ni2–D	0.173	
	Ce1–Ni2	0.286		Ce1–Ni2	0.285	Ni3–D	0.170	Ce1–Ni2	0.285	Ni3–D	0.171	
	Ni2–Ni3	0.286		Ni2–Ni3	0.285	Ni4–D	0.140	Ni2–Ni3	0.285	Ni4–D	0.151	
	Ni2–Ni4	0.249			Ni2–Ni4	0.271			Ni2–Ni4	0.285		
	Ni3–Ni4	0.249			Ni3–Ni4	0.271			Ni3–Ni4	0.285		
$24l_1$	Ce2–Ce2	0.318		Ce2–Ce2	0.392	Ce2–D	0.250	Ce2–Ce2	0.389	Ce2–D	0.299	
RT_2	Ce2–Ni1	0.294		Ce2–Ni1	0.315	Ce2–D	0.250	Ce2–Ni1	0.314	Ce2–D	0.210	
	Ce2–Ni4	0.314		Ce2–Ni4	0.470	Ni1–D	0.192	Ce2–Ni4	0.469	Ni1–D	0.196	
	Ce2–Ni4	0.285		Ce2–Ni4	0.304	Ni4–D	0.188	Ce2–Ni4	0.307	Ni4–D	0.190	
	Ni1–Ni4	0.254			Ni1–Ni4	0.344			Ni1–Ni4	0.345		
$12k_1$	Ce1–Ce2	0.344		Ce1–Ce2	0.409	Ce1–D	0.225	Ce1–Ce2	0.427	Ce1–D	0.245	
RT_2 and RT_5	Ce1–Ni4	0.321		Ce1–Ni4	0.338	Ce2–D	0.220	Ce1–Ni4	0.349	Ce2–D	0.220	
	Ce2–Ni4	0.286		Ce2–Ni4	0.304	Ni4–D	0.187	Ce2–Ni4	0.307	Ni4–D	0.189	
	Ni4–Ni4	0.248			Ni4–Ni4	0.247			Ni4–Ni4	0.244		
$4f_1$	Ce2–Ni4	0.314		Ce2–Ni4	0.470	Ce2–D	0.300	Ce2–Ni4	0.471	Ce2–D	0.304	
RT_2	Ni4–Ni4	0.248		Ni4–Ni4	0.247	Ni4–D	0.208	Ni4–Ni4	0.248	Ni4–D	0.205	
$6h$	Ce1–Ni2	0.286			Ce1–Ni2	0.285		Ce1–Ni2	0.286	Ce1–D	0.247	
RT_5	Ce1–Ni3	0.286			Ce1–Ni3	0.285		Ce1–Ni3	0.286	Ni2–D	0.143	
	Ce1–Ni4	0.320			Ce1–Ni4	0.338		Ce1–Ni4	0.349	Ni3–D	0.143	
	Ni2–Ni4	0.249			Ni2–Ni4	0.285		Ni2–Ni4	0.285	Ni4–D	0.248	
	Ni3–Ni4	0.249			Ni3–Ni4	0.285			Ni3–Ni4	0.285		

Note: The metal–deuterium bond length is 0.239 nm in CeD_2 and 0.186 nm in NiD_x.

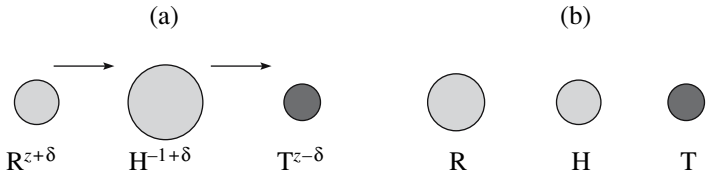

Fig. 5. Changes in atomic radii in going from (a) $CeNi_3D_{3.3}$ (RT_2 block, position $24l_1$) to (b) $CeNi_3D_{5.2}$ (RT_5 block, position $24l_2$; the radii of metal atoms are taken from [15].

the equatorial plane of the octahedron, and its center coincides with the center of the octahedral interstice.

In both deuterides, all of the deuterium sites are occupied only partially. The partial occupancy of a given site is due to the interaction between deuterium atoms in the neighboring sites (blocking), which becomes stronger with increasing deuterium content [13]. Owing to the blocking of the nearest neighbor unoccupied sites by deuterium, some of the $6h_1$ octahedral sites in the deuterium-rich deuteride are occupied.

The present results indicate that the metal–deuterium bond lengths in the highest occupancy deuterium sites $24l_2$ and $12k_1$ in the RT_5 block and between the RT_2 and RT_5 blocks (Tables 2, 3; Fig. 3) meet the "heredity" principle, proposed by Somenkov and Shilshtein [13]: the bond lengths in intermetallic deuterides are roughly equal to those in the constituent binary deuterides. At the same time, the Ni–D bond length in position $24l_1$ in the RT_2 block is increased in comparison with that in NiD_x since the transition-metal atoms are "repulsed" by the large, negatively charged deuterium atom, which accepts electrons from the rare-earth metal (Figs. 4, 5). A similar situation occurs in the case of the lower multiplicity position $4f_1$ in the RT_2 block, where the distances between the deuterium atom and the three nickel atoms shared by the RT_2 and RT_5 blocks are increased. It seems likely that this is due to the tendency of the deuterides to disproportionate (to decompose into the transition metal and stable rare-earth deuteride) on a microscopic scale, typical of RT_3 intermetallic deuterides at high temperatures. The bond-length mismatch may lead to instability of the intermetallic lattice and partial or complete amorphization of the deuteride at sufficiently high hydrogen contents, as was reported earlier for $PrNi_2H_x$ [14]. In our case, amorphization shows up as short-range ordering in the form of phase separation, evidenced by the increased intensity of small–angle neutron scattering (Fig. 2). Bond heteropolarity (the variation of the R–H and T–H bond lengths from those in the binary hydrides, due to the different charge states of hydrogen) also shows up in the hydrogen-induced volume changes and anisotropy.

It is also evident that there are different bonds between metal atoms and hydrogens in the octahedral site. The hypothetical radius of the hydrogen atoms accommodated in this site at high pressures is 0.019 nm, which is close to the covalent radius of hydrogen.

It can be seen from Table 1 that, in deuterided $CeNi_3$, the volume change per incorporated deuterium atom and the degree of anisotropy (c/a) decrease with increasing deuterium content, like in $PuNi_3$-structure deuterides [9]. Moreover, just as in $PuNi_3$-structure deuterides, the volume change and anisotropy in the $CeNi_3$-structure hydrides are smaller for heavy rare earths compared to light rare earths, as illustrated by the example of $SmRu_{1.2}Co_{1.8}$ and $SmRu_{1.6}Ni_{1.4}$ [7] (Table 1). These $CeNi_3$-structure intermetallics react with hydrogen to form hydrides with orthorhombically distorted metal matrices, weak anisotropy, and a unit-cell volume increased by 19–23%. This is due to the difference in donor properties between light and heavy rare earths: having a valence between 3+ and 4+, the former metals readily give up electrons to hydrogen [1], whereas the latter (valence between 2+ and 3+) are poorer electron donors.

The present and earlier experimental data demonstrate that the lattice distortion in deuterided (hydrided) $CeNi_3$ depends on its block structure, deuterium (hydrogen) content, and the key features of the interaction of Ce and Ni with deuterium (hydrogen).

Table 4. Radii of interstices in $CeNi_3$ and deuterium atoms in $CeNi_3D_x$

Position	Radius, nm		
	$CeNi_3$	$CeNi_3D_{3.3}$	$CeNi_3D_{5.2}$
$24l_1$	0.040	0.070	0.110
$6h_1$	0.019	0.018	0.019

CONCLUSIONS

Our neutron diffraction results show that deuterided $CeNi_3$ is isostructural with the parent intermetallic compound and has an anisotropically expanded unit cell with altered positional parameters of the metal atoms. As the deuterium content increases, the deuterium atoms occupy positions first in the structural block RT_2 and then in RT_5. At any deuterium content, all of the deuterium sites are occupied only partially because of the interaction between deuterium atoms (blocking).

Deuterium incorporation is accompanied by an increase in unit-cell volume and lattice expansion, which is anisotropic at low deuterium contents and more uniform at high deuterium contents. This behavior seems to be associated with the difference in the nature of metal–deuterium bonds, which are partially ionic for the rare-earth metal and partially metallic for the transition metal.

The deuterium-induced structural and volume changes in the RT_3 compound studied can be rationalized in terms of the heteropolarity of the M–D bond, due to the emptying of the *sp* band of the rare-earth metal and filling of the *d* band of the transition metal. The atomic radius of deuterium in the former instance is larger than that in the latter, so that deuterium, rather than the metal, can be thought to have a variable valence. The effect depends on the relationship between the R and T metals in a particular position and is best pronounced in compounds of light rare earths, which readily give up electrons, with an increase in their valence, and transition metals with an almost filled *d* band, which are incapable of accepting many electrons.

ACKNOWLEDGMENTS

This work was supported by the Russian Foundation for Basic Research, grant nos. 06-02-17062 and 06-03-33114.

REFERENCES

1. Latroche, M., Paul-Boncour, V., and Percheron-Guegan, A., Structural Properties of Two Deuterides $LaY_2Ni_9D_{12.8}$ and $CeY_2Ni_9D_{7.7}$ Determined by Neutron Powder Diffraction and X-ray Spectroscopy, *J. Solid State Chem.*, 2004, vol. 177, pp. 2542–2549.
2. Van Essen, R.H. and Bushow, K.H.J., Hydrogen Sorption Characteristics of Ce–3*d* and Y–3*d* Intermetallic Compounds, *J. Less-Common Met.*, 1980, vol. 70, pp. 189–198.
3. Burnasheva, V.V., Tarasov, B.P., and Semenenko, K.N., RNi_3–H_2 (R = Light Rare Earth) Hydrides, *Zh. Neorg. Khim.*, 1982, vol. 27, no. 12, pp. 3039–3042.
4. Yartys, V.A., New Aspects of the Structural Chemistry of Intermetallic Hydrides: "Isotropic" and "Anisotropic" Structures, *Koord. Khim.*, 1992, vol. 18, no. 4, pp. 401–408.
5. Yartys, Y.A., Isnard, O., Riabov, A.B., and Akselrud, L.G., Unusual Effect on Hydrogenation: Anomalous Expansion and Volume Contraction, *J. Alloys Compd.*, 2003, vols. 356–357, pp. 109–113.
6. Verbetsky, V.N., Klyamkin, S.N., Kovriga, A.Yu., and Bespalov, A.P., Hydrogen Interaction with RNi_3 Type Intermetallic Compounds at High Gaseous Pressure, *Int. J. Hydrogen Energy*, 1996, vols. 11–12, pp. 997–1000.
7. Shilov, A.L., Yaropolova, E.I., and Kost, M.E., Hydrides Based on SmM_3 (M = Co, Ni, Ru) Compounds, *Dokl. Akad. Nauk SSSR*, 1980, vol. 252, no. 6, pp. 1397–1400.
8. Filinchuk, Y.E. and Yvon, K., Directional Metal–Hydrogen Bonding in Interstitial Hydrides, I-$ErNi_3H_x$ ($0 < x < 3.7$), *J. Alloys Compd.*, 2005, vols. 404–406, pp. 89–94.
9. Somenkov, V.A., Lushnikov, S.A., Glazkov, V.P., and Verbetsky, V.N., Structure and Bonding Configuration of Hydrided $ErNi_3$ and $CeCo_3$, *Neorg. Mater.*, 2006, vol. 42, no. 12, pp. 1454–1463 [*Inorg. Mater.* (Engl. Transl.), vol. 42, no. 12, pp. 1326–1335].
10. Somenkov, V.A and Shilshtein, S.Sh., Hydrogen-Induced Volume Changes in Transition Metals and Intermetallic Compounds, *Fiz. Met. Metalloved.*, 1998, vol. 86, no. 3, pp. 114–122.
11. Klyamkin, S.N. and Verbetsky, V.N., Interaction of Intermetallic Compounds with Hydrogen up to 250 MPa: $LaCo_{5-x}Mn_x$–H_2 and $CeNi_5$–H_2 Systems, *J. Alloys Compd.*, 1993, vol. 194, pp. 41–45.
12. Taylor, K.N.R., Intermetallic Rare-Earth Compounds, *Adv. Phys.*, 1971, vol. 20, no. 87, pp. 551–660.
13. Somenkov, V.A. and Shilshtein, S.Sh., Structural Aspects of Behavior of Hydrogen in Metals and Intermetallic Compounds, *Phys. Chem.*, 1979, vol. 117, pp. 125–129.
14. Irodova, A.L., Goncharenko, I.N., Parshin, P.P., and Belinsan, R., Neutron Diffraction Study of Amorphous $PrNi_2D_{3.6}$, *Fiz. Tverd. Tela* (S.-Peterburg), 1996, vol. 86, no. 6, pp. 1679–1686.
15. *Spravochnik khimika* (Chemist's Handbook), Leningrad: Khimiya, 1971, vol. 1.